Nano-Sized Silica Supported $Me_2Si(Ind)_2ZrCl_2$/MAO Catalyst for Ethylene Polymerization

Kuo-Tseng Li, Cheng-Yu Li

Department of Chemical Engineering, Tunghai University Taichung, Taiwan, Republic of China

Received 12 November 2010; accepted 29 March 2011
DOI 10.1002/app.34579
Published online 11 August 2011 in Wiley Online Library (wileyonlinelibrary.com).

ABSTRACT: Nano-sized and micro-sized silica particles were used to support a zirconocene catalyst [racemic-dimethylsilbis(1-indenyl)zirconium dichloride], with methylaluminoxane as a cocatalyst. The resulting catalyst was used to catalyze the polymerization of ethylene in the temperature range of 40–70°C. Polyethylene samples produced were characterized with scanning electron microscopy (SEM), X-ray diffraction (XRD), differential scanning calorimetry (DSC), and gel permeation chromatography (GPC). Nano-sized catalyst exhibited better ethylene polymerization activity than micro-sized catalyst. At the optimum temperature of 60°C, nano-sized catalyst's activity was two times the micro-sized catalyst's activity. Polymers obtained with nano-sized catalyst had higher molecular weight (based on GPC measurements) and higher crystallinity (based on XRD and DSC measurements) than those obtained with micro-sized catalyst. The better performances of nano-sized catalyst were attributed to its large external surface area and its absence of internal diffusion resistance. SEM indicated that polymer morphology contained discrete tiny particles with thin long fiberous interlamellar links. © 2011 Wiley Periodicals, Inc. J Appl Polym Sci 123: 1169–1175, 2012

Key words: metallocene catalysts; silicas; nanoparticles; supports; polyethylene

INTRODUCTION

Polyethylene (PE) is one of the largest volume commodity chemicals produced in the world. It is used in large quantities and in many different applications, such as films, house wares, bottles, containers, pipe, tubing, wire and cable insulation, conduits, and coatings.[1,2] Ziegler-Natta catalysts, metallocene catalysts, and supported metal oxides (Philips process) all are capable of producing linear PE.[3] Metallocene catalysts activated by methylaluminoxane (MAO) show very high activity in ethylene polymerization and produce PE with a narrow molecular weight distribution of approximately two.[4,5]

Many metallocene catalysts have been supported on inorganic carriers, typically silica, for industrial use.[6–11] The development of supported metallocenes is crucial for industrial application because it enables their use in gas- and slurry-phase processes and prevent reactor-fouling problems. It also enables the formation of uniform particles with narrow size distribution and high bulk density.

In the literature, the sizes of silica particles used to support metallocene/MAO catalysts for ethylene polymerization to PE were usually in the range of micrometers where most active sites for polymerization located inside fine pores, and strong internal diffusion resistance might occur inside the pores of the micro-sized catalysts. Franceschini et al. used a commercial MAO modified micrometer-sized silica supported $Me_2Si(Ind)_2ZrCl_2$ for ethylene polymerization.[12] They found that polymers produced with the supported catalysts had lower crystallinity and higher molar mass and polydispersity values in comparison to that produced by the homogeneous one.

Nano-sized particles have a characteristic of very large external specific surface areas.[13,14] Covarrubias et al.[15] studied ethylene polymerization with bis(*n*-butylcyclopentadienyl) (denoted as cat) supported on MAO modified ZSM-2 zeolite nanocrystals (hexangonal plate-like crystal of $\sim$ 100 nm in size) and on a MAO modified commercial amorphous silica (denoted as SiO_2). They found that cat/MAO/ZSM-2 exhibited much lower polymerization activity than cat/MAO/SiO_2, and the presence of MAO on the zeolite surface had a deleterious effect on ethylene polymerization activity.

In this study, a nano-sized silica supported $Me_2Si(Ind)_2ZrCl_2$ catalyst was used for ethylene polymerization. We found that silica size had strong effect on ethylene polymerization activity, polymer molecular weight, and polymer crystallinity.

EXPERIMENTAL

Catalyst preparation and characterization

Two silica sources were used for supporting $Me_2Si(Ind)_2ZrCl_2$/MAO catalyst. One silica was

Correspondence to: K.-T. Li (ktli@thu.edu.tw).
Contract grant sponsor: National Science Council of ROC; contract grant number: NSC-97-2221-E029-028.

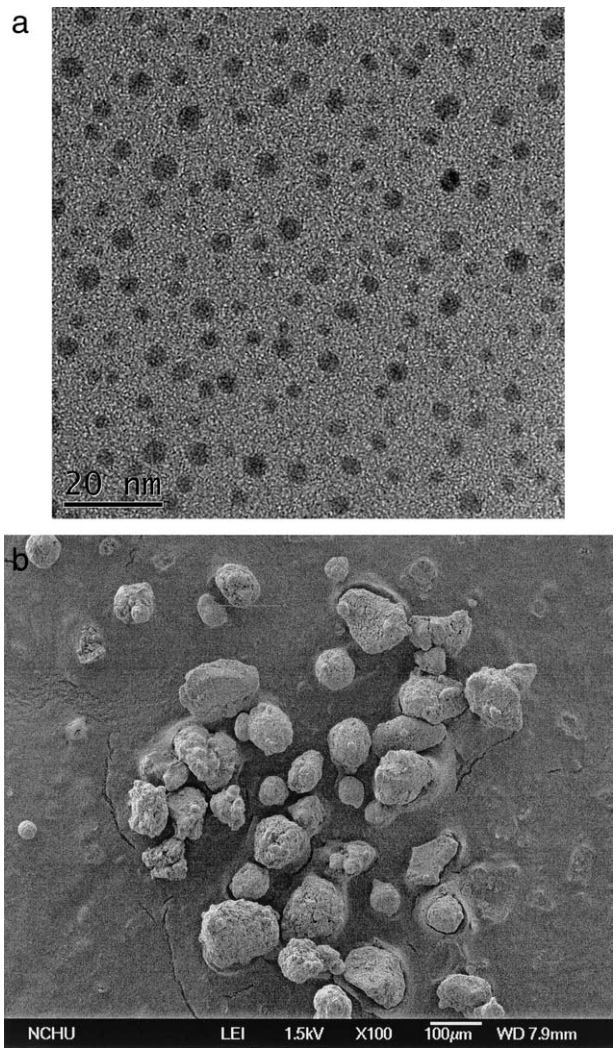

Figure 1 (a) TEM micrograph of nano-sized silica. (b) SEM micrograph of micro-sized catalyst.

nano-sized, supplied by SeedChem (Melbourne, Australia); another silica was micro-sized, supplied by Strem (Newburyport, MA). Transmission electron micrograph indicated that nano-sized silica particle had a diameter of 2–6 nm [Fig. 1(a)]. Scanning electron micrograph indicated that micro-sized silica particle had a size of around 100 μm [Fig. 1(b)].

Silica supported metallocene/MAO catalysts were prepared using a method reported earlier,[16] according to the following procedure: (1) calcination of silica particles at 450°C under a nitrogen flow (100 mL/min) for 4 h, (2) immobilization of MAO on the supports by heating 3 mL 10 wt % MAO solution (in toluene) with 0.5 g silica particle at 50°C for 24 h, followed by washing with toluene, (3) reaction of the MAO-treated supports with metallocene compounds (0.0115 g $Me_2Si(Ind)_2ZrCl_2$) at 70°C for 24 h, followed by washing with toluene, (4) drying the catalyst at 50°C. The operations of steps (2)–(4) were carried out under a dry argon atmosphere by using glove-box technique. $Me_2Si(Ind)_2ZrCl_2$ and MAO (10 wt % solution in toluene) were supplied by Strem (Newburyport, MA) and Albemarle (Baton Rouge, LA), respectively.

Zirconium contents of the resulting supported metallocene/MAO catalysts were determined with an inductively coupled plasma-atomic emission (ICP-AES) spectrometer (Kontron, Model *S*-35) after HF acid digestion of the solid. The specific surface areas of the silica samples were determined by nitrogen adsorption at the temperature of liquid nitrogen with a Micrometrics BET surface area analyzer (Model ASAP 2020).

Ethylene polymerization and polymer characterization

A 300-mL high-pressure autoclave reactor (supplied by Parr Instrumnet) equipped with an impeller and a temperature control unit was employed for carrying out the catalytic polymerization of ethylene. In a typical experiment, 100 mL toluene, 0.005 g supported $Me_2Si(Ind)_2ZrCl_2$/MAO catalysts (prepared by impregnation method mentioned above) and 3 mL MAO solution were charged to the reactor. The reactor was heated to the desired temperature (the temperature was set in the range of 40–70°C). Ethylene at 100 psi was then introduced into the reactor to initiate the polymerization and the ethylene pressure was maintained constant at 100 psi. The agitator speed was set at 400 rpm and the reaction time was 1 h. The polymerization was then terminated by adding acidic methanol and the polymer product was dried in a vacuum oven. The measured polymer weight was used for determining the polymerization activity according to the following equation: polymerization activity = (kilograms of PE)/(polymerization time × moles of Zr in the catalyst).

Polymer crystal structure was examined by X-ray diffraction (XRD) crystallography on a Shimadzu XRD-6000 diffractometer with Cu Kα radiation. Polymer particle morphology was observed using a scanning electron microscope (JEOL JSM-7000F). DSC measurements for the determination of polymer melting point (T_m) and crystallinitties (χ_C) were carried out on a differential scanning calorimeter (Perkin-Elmer Pyris-1), using a heating rate of 10 °C/min in the temperature range 30–160°C. To preserve the original PE conformation formed in the polymerization step, the DSC step for removing the heat history of PE was not performed. Percent crystallinity was calculated based upon heat of melting (fusion) = 293 J/g for 100% crystalline PE material.[17] Polymer molecular weight was determined by high-temperature gel permeation chromatography (GPC) using a Waters alliance GPCV-2000 system equipped with three columns (2 Styragel HT6E and 1 Styragel

HT2) at 135°C. *O*-dichlorobenzene was used as the mobile phase. A calibration curve was established using monodispersed polystyrene standards.

RESULTS AND DISCUSSION

Ethylene polymerization

Figure 2 shows PE yield as a function of polymerization temperature for nano-sized and micro-sized catalysts with 1 h polymerization time. It can be clearly seen from Figure 2 that nano-sized catalyst produced significantly more PE than micro-sized catalyst did. At the optimum temperature of 60°C, PE yield of nano-sized catalyst was about threefold that of micro-sized catalyst.

ICP measurements indicated that Zr contents were 0.44 wt % and 0.31 wt % for nano-sized catalyst and micro-sized catalyst, respectively. The higher Zr content of the nano-sized catalyst should be due to its larger surface area. BET measurements indicated that the nano-sized silica had a surface area of 567 m^2/g [the adsorption–desorption N_2 isotherm is shown in Fig. 3(a)], which was about two times that of the micro-sized silica (our measured surface area was 305 m^2/g,[18] and the manufacture provided surface area was $\sim$ 300 m^2/g).

For amorphous silica, the density of silanol group at a specific calcination temperature is a physical–chemical constant and is independent of the type of silica. The silanol density was reported as 2.1 OH groups/nm^2 at 450°C (our calination temperature).[19] Therefore, the content of hydroxyl group on micro- and nano-silica after calcinations was 1.06×10^{-3} mol/g and 1.98×10^{-3} mol/g, respectively. The ratio of OH (and the adsorbed MAO) is 1.87, which is slightly higher than the Zr content ratio (= 1.42).

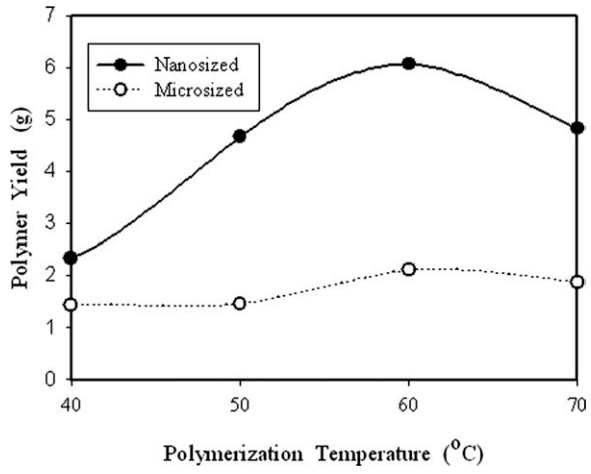

Figure 2 Polymer yield as a function of polymerization temperature for (a) nano-sized catalyst and (b) micro-sized catalyst.

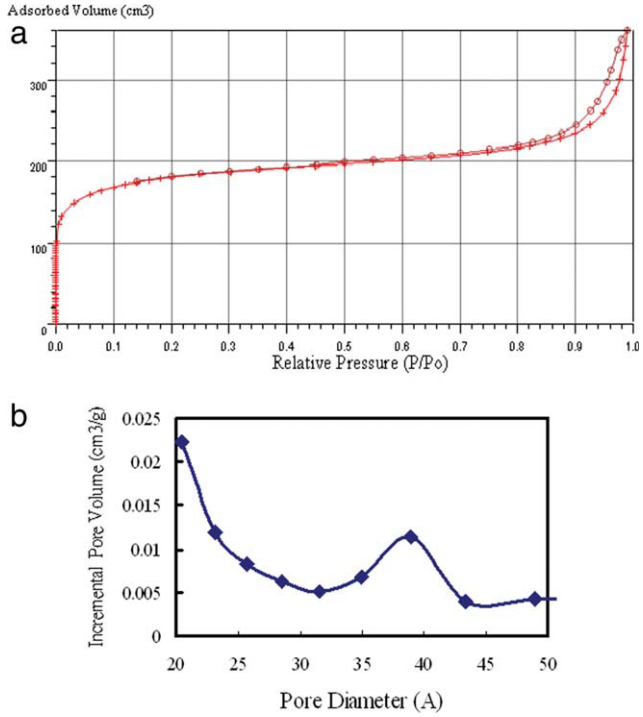

Figure 3 (a) Adsorption–desorption N_2 isotherm of nano-sized catalyst. (b) Pore size distribution of nano-sized silica. [Color figure can be viewed in the online issue, which is available at wileyonlinelibrary.com.]

Figure 3(b) shows the pore size distribution of nano-sized silica, which was obtained form the desorption curve (the upper curve) of Figure 3(a). The pore size distribution of the micro-sized catalyst was given elsewhere.[18] Figure 3(b) indicates that most pores in nano-sized catalysts were less than 2 nm (by IUPAC recommended classification, pores less than 2 nm in width are termed micropores[20]). TEM picture (Fig. 1) also indicates that the pore size in nano-sized catalysts was very small. Our previous data show that almost all pores in micro-sized catalyst were in the range of 10–30 nm with an average pore diameter of around 22 nm. The pore volume of nano-sized catalyst was 0.35 cm^3/g, which was only 22% of the micro-sized catalyst pore volume (1.6 cm^3/g).

Based on the Zr content data, specific polymerization activities were calculated and the results are presented in Figure 4. The specific polymerization activities were expressed as kg PE/mol Zr h (i.e., based on the same amount of Zr), therefore, the difference of Zr content in nano-sized catalyst and micro-sized catalyst had no effect on the specific catalyst activity. Curves in Figure 4 exhibit a volcano shape with a maximum polymerization activity at the polymerization temperature of 60°C. Below and above the optimum temperature, polymerization activity decreased. In Figure 4, the maximum polymerization activities obtained for nano-sized catalyst

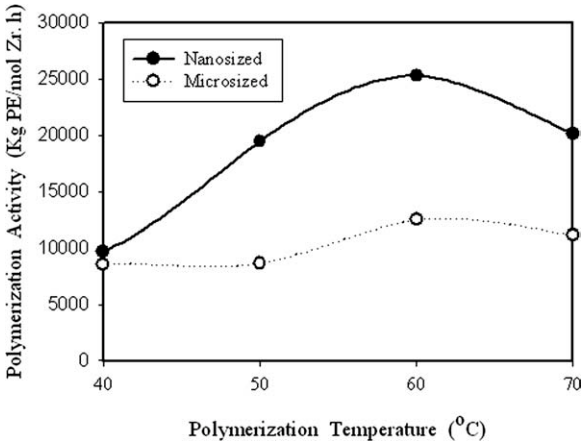

Figure 4 Polymer activity as a function of polymerization temperature for (a) nano-sized catalyst and (b) micro-sized catalyst.

and micro-sized catalyst were 2.53×10^4 kg PE/mol Zr h and 1.25×10^4 kg PE/mol Zr h, respectively. That is, the maximum activity obtained (at 60°C) with nano-sized catalyst was 2.02 times that obtained with micro-sized catalyst.

The global polymerization rate, R_p, in metallocene catalysis, is generally represented by[18,21]:

$$R_p = k_p[\mathrm{C}^*]\cdot[\mathrm{M}] \quad (1)$$

where k_p is propagation rate constant, $[\mathrm{C}^*]$ is active species concentration, and [M] is monomer concentration. $[\mathrm{C}^*]$ in eq. (1) is related to polymerization time t.[22]

$$[\mathrm{C}^*] = [\mathrm{C}^*]_\mathrm{o} \exp(-k_d\, t) \quad (2)$$

where $[\mathrm{C}^*]_\mathrm{o}$ is the initial concentration of catalytic active species, k_d is deactivation constant.

The volcano shape in Figure 4 might be attributed to increase in the rates of both propagation ($k_p = k_{p0}\exp[-E_p/RT]$) and catalyst deactivation ($k_d = k_{d0}\exp[-E_d/RT]$) with increasing temperature. In addition, ethylene solubility in toluene [[M] in eq. (1)] decreased rapidly with increasing temperature.[23]

Figure 4 also indicates that the polymerization activity of nano-sized catalyst was more sensitive to the temperature change than that of micro-sized catalyst. This suggested that micro-sized catalyst had strong diffusion resistance because diffusion coefficient is less sensitive to temperature change than intrinsic polymerization rate constant. For the case of strong internal diffusion limitation, the apparent activation energy was equal to 1/2 the true activation energy.[24]

Most of the nano-sized slica surface area was external surface area, and active sites on the nano-sized catalyst external surface should be free from internal diffusion resistance. On the contrary, most of micro-sized slica surface area was internal (i.e., inside the pores), and active sites on the internal surface might have strong diffusion resistance. Therefore, nano-sized catalyst's active sites had higher ethylene concentration than micro-sized catalyst's active sites, which resulted in the higher polymerization rate [according to eq. (1)] for the former, as shown in Figure 4.

Polymer characterization

Figure 5 shows polymer weight-averaged molecular weight (denoted as $\overline{M_w}$) as a function of polymerization temperature. Under identical polymerization conditions, nano-sized catalyst produced PE with significantly higher molecular weight than micro-sized catalyst did. Figure 5 also shows that the molecular weight of the polymer produced decrease with increasing polymerization temperature (T_P). For nano-sized catalyst produced polymer, $\overline{M_w}$ decreased from 2.74×10^5 to 1.51×10^5 g/g mol when T_P increased from 40 to 70°C.

For a homogeneous polymerization catalyst, it was proposed that

$$1/\overline{P}_n = (k_{\mathrm{TM}}/k_P)\ (1/[\mathrm{M}]) + k_{\mathrm{TO}}/k_p \quad (3)$$

where $\overline{P_n}$ is degree of polymerization (= number-averaged molecular weight/monomer molecular weight), [M] is monomer concentration, k_P is propagation rate constant, k_{TM} is chain termination rate constant due to β-H transfer to the metal, and k_{TO} is chain termination rate constant due to β-H transfer to an olefin.[25]

Equation (3) indicates that the higher monomer concentration [M], the higher molecular weight of the polymer produced. Therefore, the higher molecular weight observed for the polymer produced with

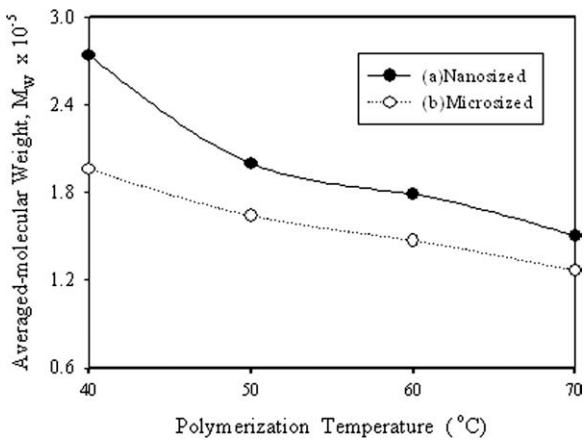

Figure 5 Effect of polymerization temperature on molecular weight of polyethylene produced with (a) nano-sized catalyst and (b) micro-sized catalyst.

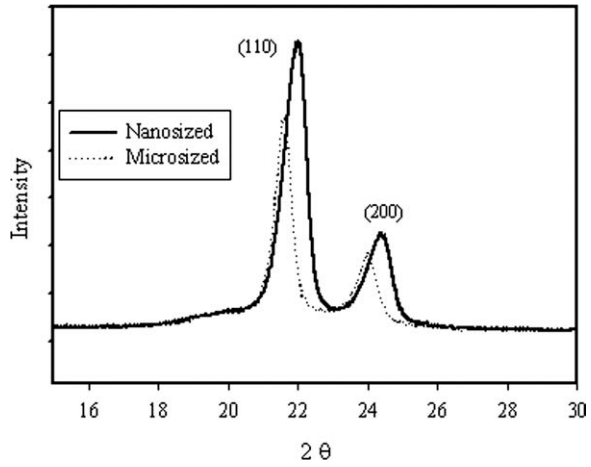

Figure 6 Comparison of X-ray powder diffraction (XRD) patterns for polyethylene produced with nano-sized catalyst and micro-sized catalyst.

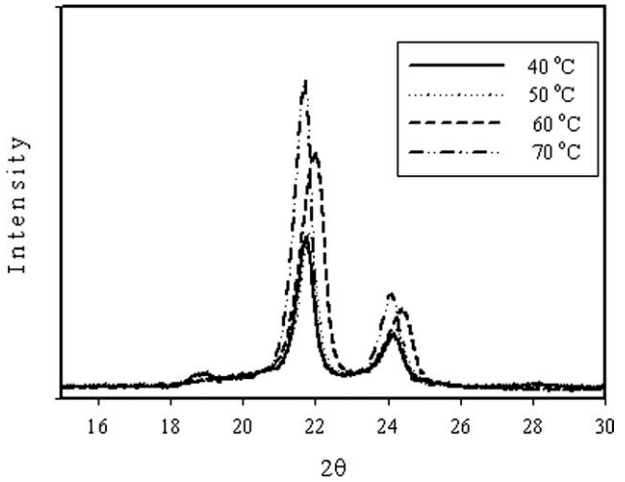

Figure 7 Effect of polymerization temperature on polyethylene XRD patterns obtained with nanosized catalyst.

the nano-sized catalyst (Fig. 5) should be caused by the higher monomer concentration at the active sites of the nano-sized catalyst. As mentioned above, nano-sized catalyst's active sites were located at the external surface and had no internal diffusion resistance; micro-sized catalyst's active sites were located inside the pores and had strong internal diffusion resistance. Therefore, the external active sites on nano-sized catalyst had higher monomer concentration than the internal active sites on micro-sized catalyst, and thus produced polymers with higher molecular weight.

The decrease of molecular weight with increasing polymerization temperature (shown in Fig. 5) should be due to the enhanced chain-transfer reactions. That is, k_{TM}/k_P or k_{TO}/k_p increased with increasing polymerization temperature because the activation energies for chain-transfer reactions (E_{TM} and E_{TO}) are greater than the activation energy for propagation reaction (E_P).[18]

Figure 6 shows wide-angle X-ray diffraction (XRD) spectra of PE produced with nano-sized catalyst and micro-sized catalyst (polymerization temperature = 60°C), which indicates that the former has much stronger intensity than the latter. The spectra exhibit (1,1,0) and (2,0,0) diffraction peaks of PE, indicating that the samples had orthorhombic crystal structure.[26]

Figure 7 shows the effect of polymerization temperature on polymer XRD spectra, which indicates that XRD peak intensity increases significantly with increasing polymerization temperature. In Figures 6 and 7, the sharp peaks are due to the scattering from the crystalline regions and the broad underlying "hump" is due to scattering from noncrystalline areas.[27] The degree of crystallinity (χ_c) was calculated from XRD spectra in Figure 7 according to the following equation:

$$\chi_c = A_c/(A_c + A_a) \quad (4)$$

where A_a is the area under the amorphous hump and A_c is the area remaining under the cryatalline peaks. The calculation results are shown in Figure 8, which indicates that PE samples produced with nano-sized catalyst had significantly higher degree of crystallinity than those produced with micro-sized catalyst. At the polymerization temperature of 60°C, polymer produced with nano-sized catalyst had a crystallinity of 70%, which was comparable with the crystallinity of commercial HDPE products (crystallinity = 70–90%).[28]

Figure 9 shows the degree degree of crystallinity (χ_c) determined with differential scanning calorimetry (DSC), which also indicates that PE samples produced with nano-sized catalyst had significantly

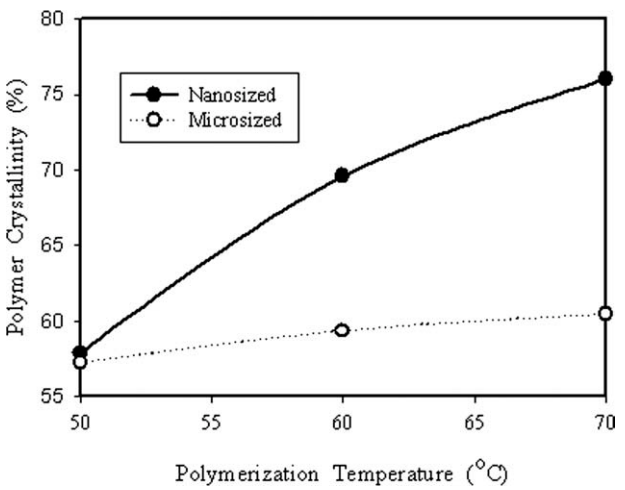

Figure 8 Degree of crystallinity (obtained with XRD measurements) as a function of polymerization temperature for polymers produced with nano-sized and micro-sized catalyst.

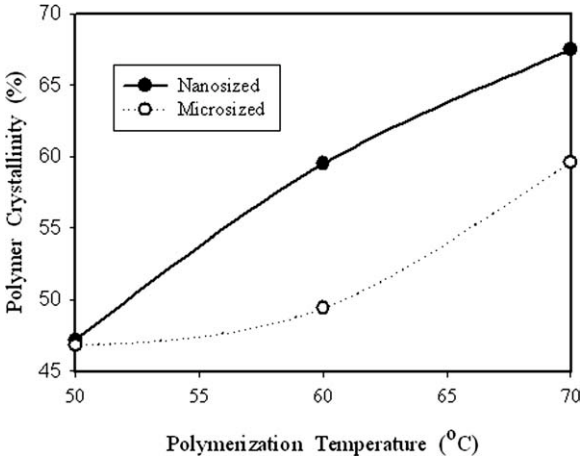

Figure 9 Degree of crystallinity (obtained with DSC measurements) as a function of polymerization temperature for polymers produced with nano-sized catalyst and micro-sized catalyst.

higher degree of crystallinity than those produced with micro-sized catalyst.

In crystals, PE folds back and forth along the backbone of the chain. Something on the order of 40 segments exist in the fully extended form in these crystals before the chain folds back on itself and repeats the process.[29] For nano-sized catalyst, most polymers were produced at the active sites located at the catalyst external surface, which had more space for polymers to fold into crystals. For micro-sized catalyst, most polymers were produced at the active sites located in the pores of micro-sized catalyst. The internal surface had limited space for polymers to fold into crystal structure. Therefore, polymers produced with nano-sized catalyst had higher degree of crystallinity than those produced with micro-sized catalysts, as shown in Figures 8 and 9.

Figures 8 and 9 also indicate that degree of crystallinity increased with increasing polymerization temperature. This might be due to the decrease of molecular weight at the higher polymerization temperature. It is known that the degree of crystallinity increases with decreasing the molecular weight of the polymer chains.[30]

Polydispersity ($=\overline{M_w}/\overline{M_n}$) of our PEs was in the range of 1.4–1.9 (shown in Table I), which was much lower than the PE polydispersity in Franceschini et al.[12] (their $\overline{M_w}/\overline{M_n}$ values ranged from 4 to 6.9 for supported catalysts). The results indicate that our PEs had narrower molecular distribution than those in Franceschini et al. Table I also shows that melting temperatures (T_m) of the PEs obtained with nano-sized silica supported $Me_2Si(Ind)_2ZrCl_2$/MAO catalyst was in the range of 132–138°C, which was lower than the melting temperature obtained previously with nano-sized silica supported Cp_2ZrCl_2/MAO catalyst ($T_m \sim 139$°C).[13] The lower T_m means lower molecular weight, therefore, it is possible to produce PE with bimodal molecular weight distribution using a Cp_2ZrCl_2-$Me_2Si(Ind)_2ZrCl_2$ mixed catalyst system supported on nano-sized silica. For highly crystalline HDPE samples, the reported melting points were in the range of 133–138°C.[1]

TABLE I
Polydispersity ($= \overline{M_w}/\overline{M_n}$) and Melting Temperature (T_m) of HDPE Obtained with Nano-Sized Catalyst

Polymerization temperature	40°C	50°C	60°C	70°C
Polydispersity	1.4	1.9	1.8	1.6
T_m (°C)	138.5	136.0	135.3	132.8

Figure 10(a,b) shows SEM photos of PE produced with nano-sized catalyst and with micro-sized silica, respectively. The PE morphology in Figure 10(a) is different from that in Figure 10(b). The polymer molecules in Figure 10(a) were mainly in two forms: discrete tiny particles and long thin fibers, and the morphology of the obtained PE tiny particles similar to that of nano-sized support, shown in Figure 1(a).

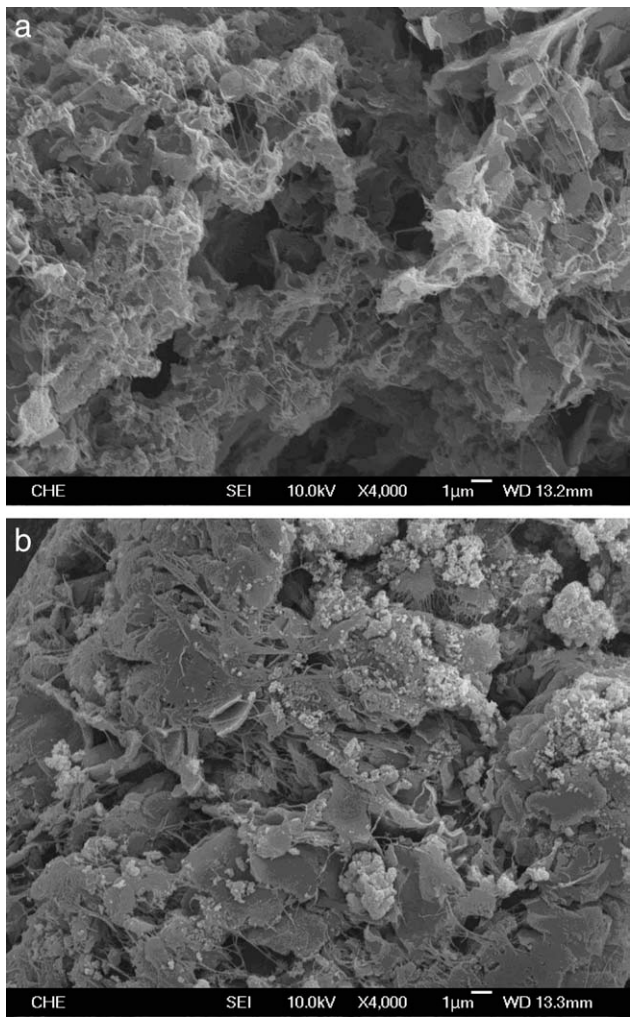

Figure 10 (a) SEM micrograph of polyethylene produced with nano-sized catalyst at 70°C. (b) SEM micrograph of polyethylene produced with micro-sized catalyst at 70°C.

CONCLUSIONS

A nano-sized silica supported $Me_2Si(Ind)_2ZrCl_2$/MAO catalyst was prepared by impregnation of $Me_2Si(Ind)_2ZrCl_2$ on a MAO-modified silica support. At the optimum polymerization temperature of 60°C, the polymerization activity of nano-sized catalyst was 2.02 times that obtained with micro-sized catalyst. Polymers produced with nano-sized catalyst had higher molecular weight than those produced with micro-sized catalyst. The superiority of the nano-sized catalyst should be caused by the fact that most of its active sites were located at the exterior surface, which was free from internal diffusion resistance. XRD and DSC measurements indicated that polymers produced with nano-sized catalyst had significantly higher crystallinity than that produced by the micro-sized catalyst. SEM studies indicated that the resulting polymer contained tiny particles with a dispersion of thin fiberous intercrystalline links, and the morphology of the obtained PE tiny particles similar to that of nano-sized support.

References

1. Beach, D. L., Kissin, Y. V. In Encyclopedia of Polymer Engineering and Science; Mark, H. F.; Bikales, N. M.; Overberger, C. G.; Menges, G., Eds.; Wiley: New York, 1986; Vol.6, p 454.
2. James, D. E. In Encyclopedia of Polymer Engineering and Science; Mark, H. F.; Bikales, N. M.; Overberger, C. G.; Menges, G., Eds.; Wiley: New York, 1986; Vol.6, p 429.
3. Kissin, Y. V. In Encyclopedia of Chemical Technology, 4th ed.; Kroschwitz, J. I.; Howe-Grant, M., Eds.; Wiley: New York, 1996; Vol. 17, p 735.
4. Kaminsky, W. J Polym Sci Part A Polym Chem 2004, 42, 3911.
5. Kaminsky, W.; Laban, A. Appl Catal A 2001, 222, 47.
6. Sinn, H. W.; Kaminsky, W.; Vollmer, H. J.; Woldt, R. (to BASF). U.S. Pat. 4,403,344 (1983).
7. Kaminsky, W.; Hahnsen, H.; Kulper, K.; Woldt, R. (to Hoechst) U.S. Pat. 4,542,199 (1985).
8. Ribeiro, M. R.; Deffieux, A.; Portela, M. F. Ind Eng Chem Res 1997, 36, 1224.
9. Chien, J. C. Top Catal 1999, 7, 23.
10. Kristen, M. O. Top Catal 1999, 7, 89.
11. Hlaty, G. G. Chem Rev 2000, 100, 1347.
12. Franceschini, F. C.; Tavares, T. T.; Bianchini, D.; Alves, M. C.; Ferreira, M. L.; dos Santo, J. H. Z. J Appl Polym Sci 2009, 112, 563.
13. Li, K. T.; Dai, C. L.; Kuo, C. W. Catal Commun 2007, 8, 1209.
14. Li, K. T.; Ko, F. S. J Appl Polym Sci 2008, 107, 1397.
15. Covarrubias, C.; Quijada, R.; Rojas, R. Appl Catal A 2008, 347, 223.
16. Chien, J. C.; He, D. J Polym Sci Part A Polym Chem 1991, 29, 1603.
17. Blaine, R. L. http://www.tainstruments.co.jp/application/pdf/Thermal Library/Application _Notes/TN048.PDF.
18. Li, K. T.; Kao, Y. T. J Appl Polym Sci 2006, 101, 2573.
19. Zhuravlev, L. T. Colloids Surf A 2000, 173, 1.
20. Satterfield, C. N. Heterogeneous Catalysis in Industrial Practice, 2nd ed.; McGraw-Hill: New York, 1991; p 143.
21. Lieberman, R. B.; Barbe, P. C. In Encyclopedia of Polymer Engineering and Science; Mark, H. F.; Bikales, N. M.; Overberger, C. G.; Menges, G., Eds.; Wiley: New York, 1988; Vol. 13, p 464.
22. Meier, G. B.; Weickert, G.; van Swaaij, W. P. M. J Appl Polym Sci 2001, 81, 1193.
23. Atiqullah, M.; Hammawa, H.; Hamid, H. Eur Polym Mater 1998, 34, 1511.
24. Fogler, H. S. Elements of Chemical Reaction Engineering, 4th ed.; Prentice Hall: Upper Saddle River, NJ, 2006; p 834.
25. Stehling, U.; Diehold, J.; Kirsten, R.; Roll, W.; Brintzinger, H.; Jungling, S.; Mulhaupt, R.; Langhauser, F. Organometallics 1994, 13, 964.
26. Krimm, S.; Tobolsky, A. V. J Polym Sci 1951, 7, 57.
27. Young, R. J.; Lovell, P. A. Introduction to Polymers, 2nd ed.; Chapman & Hall: London, 1991; p 266.
28. Doak, K. W. In Encyclopedia of Polymer Engineering and Science; Mark, H. F.; Bikales, N. M.; Overberger, C. G.; Menges, G., Eds.; Wiley: New York, 1986; Vol. 6, p 384.
29. Hiemenz, P. C. Polymer Chemistry; Mercel Dekker: New York, 1984; p 63.
30. Nunes, R. W.; Martin, J. R.; Johnson, J. F. Polym Eng Sci 1982, 22, 205.